Absorption Equilibrium and Kinetics for Ethylene-Ethane Separation with a Novel Solvent

Travis A. Reine, R. Bruce Eldridge

Introduction

The separation of olefins and paraffins is of primary importance in the chemical industry. The production of polymers and other specialty chemicals from mono-olefins such as ethylene requires the olefin to be of extremely high purity (>99.9%).[1] In order to achieve such a high degree of separation from the close boiling point mixture of ethylene/ethane, distillation towers with an enormous number of trays are operated at high pressures and cryogenic temperatures (between -40ºC and -90ºC). At these cryogenic temperatures, closed heat loops are often used with ethylene or propylene as the working fluid. Even with the high level of heat integration present in a modern ethylene unit, the energy expenditure is enormous making up 6.2% of the total yearly energy requirement of all distillation processes.[2] Despite the high capital and energy costs associated with cryogenic distillation, it has remained the dominant technology for light olefin/paraffin separations for many years because of its proven effectiveness and reliability. The method of olefin/paraffin separation certainly holds an enormous potential for capital and energy cost savings if a more efficient technique is developed. Many alternatives have been investigated including extractive distillation, absorption, adsorption, and membranes.[3] Chemical absorption possesses the most attractive characteristics of the gas-liquid processes, but an in-depth study into the equilibrium and kinetics of the absorption of ethylene is lacking in the literature. By using a stirred-cell for measuring ethylene uptake, equilibrium and kinetic data were acquired for a novel absorption solution comprised of traditional organic solvents and CuCl.

Experimental

The setup for the autoclave experiments is shown in Figure 1 following absorption experimental techniques common in the literature.[4,5] The basic equipment was a 1 gallon, stainless steel vessel used to transfer a known amount of gas into a 500 cc stainless steel autoclave for gas-liquid contacting. The gases used in the autoclave experiments were chemically pure grade ethylene (99.5%) and ethane (99.0%) from Air Liquide.
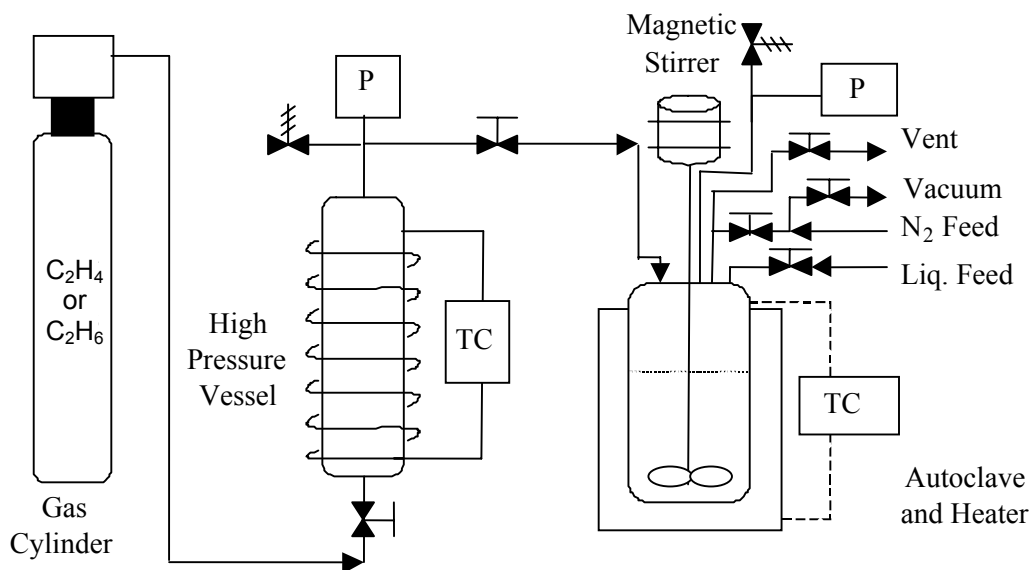
Figure 1. Autoclave apparatus experimental setup

To begin an absorption experiment, a weighed amount of liquid was added to the autoclave, and pure gas from the high pressure vessel was added while recording the initial conditions. After the gas was charged, the stirrer was turned on and measurements were taken at very short intervals (i.e. every 10 to 15 seconds). Typical stirrer speeds for the kinetic experiments (between 100 and 300 r.p.m.) were much lower than the equilibrium experiments (between 600 and 800 r.p.m.) because higher stirrer speeds caused distortions in the flatness of the liquid interfacial area. As the change in autoclave pressure with time decreased due to the system approaching equilibrium, the pressure and temperature readings were taken less frequently. Eventually, a steady condition was obtained where the pressure no longer changed as seen in Figure 2 for the pressure reading with time for a particular experiment. Once the final equilibrium conditions were recorded, the stirrer was stopped and the solution was either regenerated or kept for a subsequent absorption or desorption experiment.
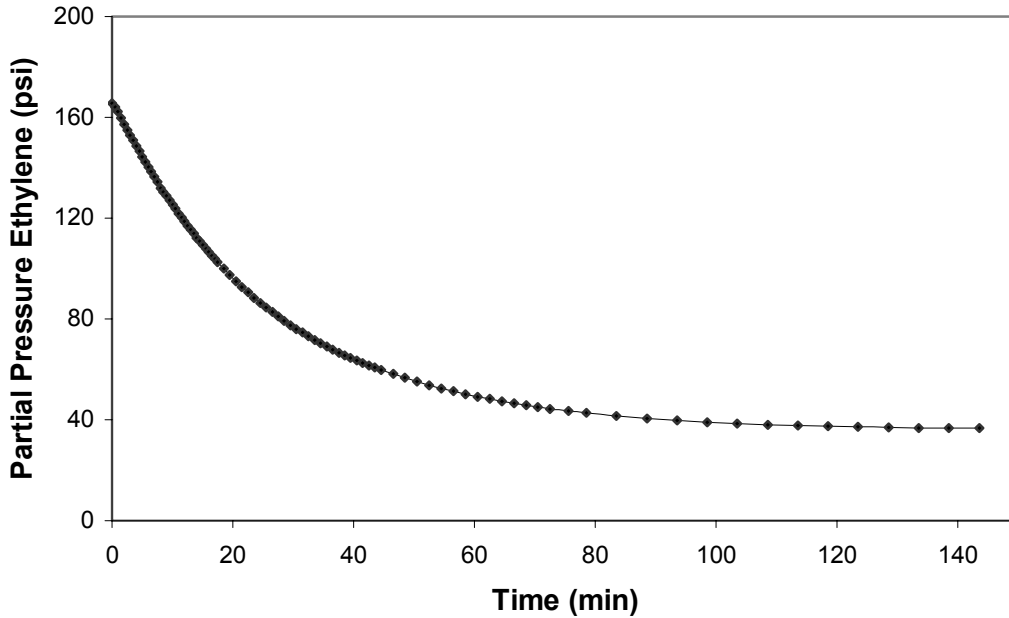
Figure 2. Pressure profile of a typical ethylene absorption experiment

In order to calculate the amount of absorbed gas at equilibrium or at any time during the experiment, the following assumptions were made: (1) The absorption liquid was nonvolatile at the absorption conditions. At ambient temperature the total vapor pressure contribution of the liquids is less than 0.01 psi. (2) The amount of absorbed gas in the initial liquid was negligible. Comparison of equilibrium results from fresh and regenerated solutions showed this to be a good approximation. (3) There was no gas phase mass transfer resistance. The experiments were performed with pure absorption gases. With these assumptions, a mass balance was used to relate initial moles of gas in the charged autoclave with moles of gas in the vapor space at any given time during the experiment.

$$n_{absorbed} = n_{autoclave,\,charged} - n_{autoclave,\,time} \tag{1}$$

$$n_{absorbed} = \frac{V_{autoclave}}{R}\left(\left(\frac{P}{ZT}\right)_{autoclave,\,charged} - \left(\frac{P}{ZT}\right)_{autoclave,\,time}\right) \tag{2}$$

The compressibility, Z, was calculated for each condition by the three-parameter Prausnitz and Pitzer correlation as developed by Smith, Van Ness, and Abbott.[6]

Results and Discussion
Equilibrium

Each absorption experiment from a particular gas charge produced an equilibrium value of gas concentration in the liquid at a given gas partial pressure. A compilation of multiple experiments over a range of gas charges yielded the equilibrium behavior of the absorption gas. Figure 3 shows that the CuCl absorption solution has a much higher capacity for ethylene than ethane. The trendline through the ethane equilibrium data was fitted with a y-intercept of zero, and the R^2 value of the line was 0.996 with a slope of 0.00201 mol·(L psia)$^{-1}$. For physical solubility, the Henry's law constant can be defined as

$$m = \frac{c^*}{P^*} \tag{3}$$

where c is concentration of the gas in the liquid phase, P is the partial pressure of the gas, and the * superscript refers to the equilibrium condition. The ethylene in CuCl solution equilibrium data was definitely not described by Henry's law; in fact, the solution still had an ethylene capacity over 0.45 M at atmospheric pressure.
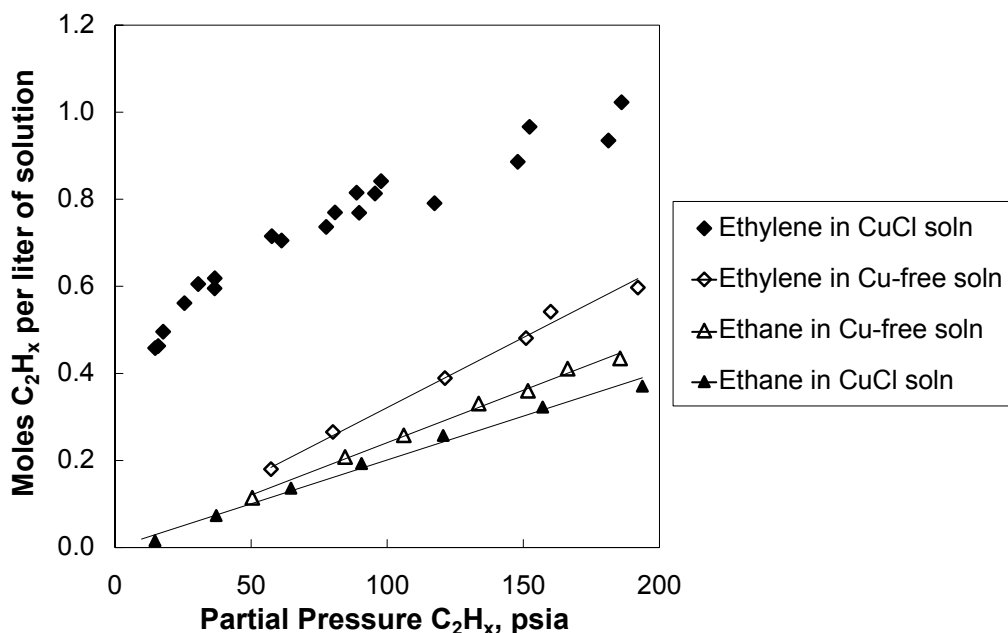

Figure 3. Ethylene and ethane equilibrium with CuCl and Cu-free solutions

In order to determine how much of the ethylene absorption was due to physical solubility in the liquid, a copper-free solution was prepared with the liquids in the same molar ratio as in the CuCl case. Comparison of equilibrium data obtained for this solution with ethylene and ethane in Figure 3 showed that the copper-free solution had higher capacity for ethylene over ethane. The ethylene capacity of the copper-free solution was much lower than the copper case suggesting that chemical effects were indeed important. Like ethane in CuCl solution, both ethylene and ethane with the copper-free solution showed absorption equilibrium following Henry's law. For ethylene, the R^2 value of the line was 0.993 with a slope of 0.00322 mol·(L psia)$^{-1}$. For ethane, R^2 value of the line was 0.997 with a slope of 0.00245 mol·(L psia)$^{-1}$.

With ethane, the copper-free solution demonstrated higher solubility than the CuCl solution; therefore, a salting-out effect was observed. Since the CuCl solution exhibited a very high olefin capacity, the decrease in paraffin solubility due to the presence of the CuCl resulted in a greater improvement in selectivity than if the salting-out had not occurred. Selectivity is defined here as the ratio of ethylene absorbed to ethane absorbed at equilibrium.

$$selectivity = \frac{c^*_{total}}{m_{ethane} P^*} \tag{4}$$

For the copper-free solution, the ratio of the solubilities of the gases was 1.3, which was independent of pressure. Taken to much higher pressures, the liquid eventually became saturated with the gas, but for gas pressures less than ~150 psia, no deviation from Henry's law was found.

In order to account for CuCl effects and estimate the degree of physical solubility of ethylene with the copper solution, an analogy with the non-reactive cases was used. This technique called the N_2O analogy in CO_2 absorption is commonly employed to find the solubility of CO_2 in an amine solution.[7] Usually the CO_2 solubility is found by assuming that the ratio of the solubility of the reactive gas (CO_2) to the non-reactive gas (N_2O) in a non-reactive liquid (water) is the same as the ratio of the solubility of these gases in the reactive liquid (amine solution). The copper-free solution referred to with *non-Cu* subscript in the following equation was the non-reactive solution in the analogy.

$$m_{\text{ethylene Cu}} = \frac{m_{\text{ethylene non-Cu}} \cdot m_{\text{ethane Cu}}}{m_{\text{ethane non-Cu}}} \tag{5}$$

$$m_{\text{ethylene Cu}} = \frac{(0.00322)(0.00201)}{0.00245} = 0.00264 \frac{\text{mol}}{\text{L} \cdot \text{psia}} \tag{6}$$

In order to successfully describe the absorption process, an equilibrium model was developed based on the simple first-order reaction.

$$Cu^+ + C_2H_4 \leftrightarrow Cu^+(C_2H_4) \tag{7}$$

where the equilibrium constant is defined by

$$K_{eq} = \frac{\left[Cu^+(C_2H_4)\right]}{\left[Cu^+\right]\left[C_2H_4\right]} \tag{8}$$

where the activity coefficients are neglected here for simplification. In fact, for concentrated reactive absorption systems, the use of activity coefficients is generally superfluous and can lead to substantial errors when calculating equilibrium and rate constants for different solution compositions.[8]

The concentration of dissolved ethylene in equation (8) is given by using the solubility from equation (6) with equation (3). The concentration of copper:ethylene complex is found by subtracting the calculated physical solubility from the total ethylene concentration in the liquid for each equilibrium point. The resulting ethylene absorption was entirely due to chemical complexation with copper.

$$c^*_{\text{chemical}} = c^*_{\text{total}} - P^* m_{\text{ethylene Cu}} \tag{9}$$

The concentration of free copper can be found by a total copper balance, and equation (8) can be rewritten as

$$K_{eq} = \frac{c^*_{\text{total}} - mP^*}{\left(c_{\text{Cu total}} - c^*_{\text{total}} + mP^*\right)\left(mP^*\right)} \tag{10}$$

where $c_{\text{Cu total}}$ is the total copper concentration, and m is the calculated Henry's law constant for the ethylene in copper case, $0.00264 \text{ mol} \cdot (\text{L psia})^{-1}$. $c_{\text{Cu total}}$ was found by flame atomic absorption to be 1.13 M, but it will be treated as an unknown to allow the model freedom to fit the data. Rearrangement of equation (10) in order to find the unknowns K_{eq} and $c_{\text{Cu total}}$ yields the following linear equation

$$\frac{c^*_{\text{total}}}{mP^*} = -K_{eq}\left(c^*_{\text{total}} - mP^*\right) + \left(1 + K_{eq} \cdot c_{\text{Cu total}}\right) \tag{11}$$

where the slope is $-K_{eq}$ and the y-intercept is $1 + K_{eq} \cdot c_{\text{Cu total}}$. Figure 4 shows the linear fit to this equation of the equilibrium data points below 100 psia. The R^2 value of the linear fit was

0.888 and the value of K_{eq} from the slope of the line was 45.2 L/mol. The calculated value of the total copper concentration was 0.65 M, which was 58% of the actual value of 1.13 M.
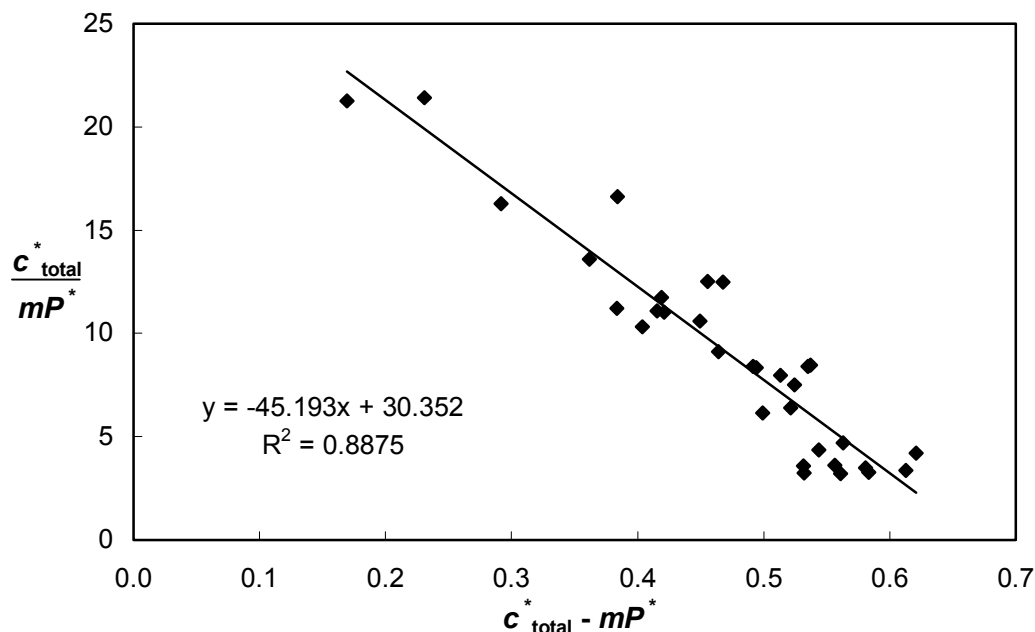

The chart shows a y-axis labeled $\dfrac{c^*_{total}}{mP^*}$ ranging from 0 to 25, and an x-axis labeled $c^*_{total} - mP^*$ ranging from 0.0 to 0.7. The equation shown on the plot is:

$$y = -45.193x + 30.352$$
$$R^2 = 0.8875$$

Figure 4. Linear fit for first-order equilibrium model

The ethylene absorption from the first-order equilibrium model is shown to fit the data very well in Figure 5. A comparison of the physical and chemical effects is also shown in Figure 5. Examining the total ethylene absorption at pressures over ~40 psia revealed that the slope of the equilibrium data was nearly the same as the calculated physical solubility. As a result, the calculated chemical absorption plateaued around 40 psia at an ethylene concentration around 0.58 M in the liquid. With the chemical absorption reaching an asymptotic limit, the copper solution is fully loaded chemically, and higher pressures result only in increased physical absorption. Since the copper concentration was 1.13 M, this would lead to the assumption that about half of the copper in solution participates in a 1:1 complex with ethylene. This could be a result of coordinating ligand strength that inhibits the ethylene exchange equilibrium or a result of partial degradation of the copper(I) state due to oxidation. Another possibility is that all of the copper(I) is active and forms a 2:1 complex with ethylene; however, this theory was discounted from experimental data with other ligands.
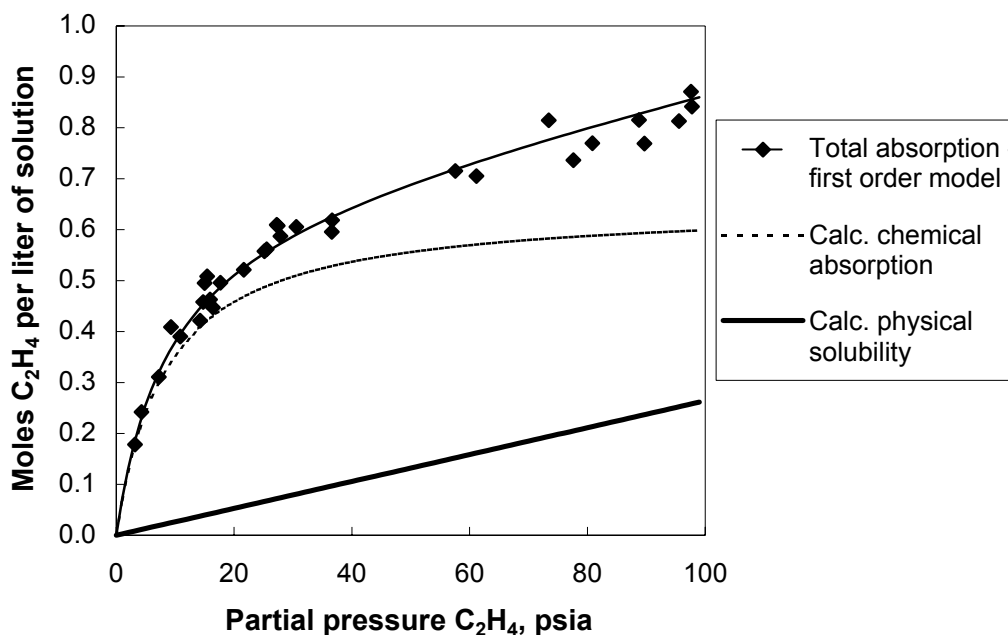
Figure 5. Calculated chemical and physical equilibrium

For the copper solution, the selectivity defined by equation (4) was highest at the lowest gas pressures because the physical solubility effects were dominated by the chemical complexation effects. At atmospheric pressure, the pure gas selectivity was about 15. At partial pressures over about 40 psia, the selectivity is much lower due to the fact that the copper sites are becoming saturated while the physically solubility remains unchanged. A tradeoff existed for ethylene absorption and operating pressure such that higher pressures led to higher ethylene capacity but lower selectivity and lower pressures led to higher selectivity and lower capacity. The maximum ethylene/ethane selectivity was found at vacuum pressures, but the low ethylene capacity at low pressures would be prohibitory to optimum process design. Since the extent of the chemical effects was observed to be around 40 psia in Figure 5, this ethylene pressure should be the maximum operating partial pressure. Higher selectivities can be realized at lower pressures at the expense of absorption capacity.

Kinetics

Stirred cells have been used frequently in the literature for gas absorption, and the experimental technique of operating the gas and liquid batchwise to obtain kinetic information has been demonstrated by Jamal and Meisen[4] and Xu et al.[9] By charging pure absorption gas and recording the pressure decrease, investigators have calculated reaction coefficients for appropriate models to fit the experimental data. In a similar manner, this present study compared the fitting capability of five different kinetic models to determine which model best described the experimental data. In developing a kinetic expression for ethylene absorption, the film theory is assumed to be valid for the system to simplify the calculations. Danckwerts[8] has shown that for most cases of gas absorption with chemical reaction, the simple film theory provides equivalent accuracy to the other more complicated models like penetration theory and surface renewal theory. In order to solve for the concentration of each component in the liquid phase, the following key assumptions about the interfacial and bulk concentrations were necessary as shown schematically in Figure 6.

The interfacial concentration of ethylene in the liquid is given by the physical solubility in equilibrium with the gas phase ethylene pressure. From the calculated Henry's law constant in equation (6), the uncomplexed ethylene concentration at the interface is given by

$$c_{A,i} = m_{\text{ethylene Cu}} P \tag{12}$$

where P is the measured pressure, which is a function of time. For simplicity, the complexation reaction (7) is rewritten as

$$A + B \xleftrightarrow{k_1, k_2} C \tag{13}$$

where k_1 and k_2 are forward and reverse reaction rate coefficients, respectively, A is uncomplexed ethylene, B is copper not complexed to ethylene, and C is the copper-ethylene complex. The reaction is assumed to occur exclusively in the film of thickness x_L, so that in the bulk of the liquid there is no more reaction proceeding. This assumption leads to the requirement that the bulk liquid is in equilibrium. For the kinetic experiment, the total concentration of ethylene in the liquid c_{total} is the measured value as a function time. Since a model describing the equilibrium for reaction (13) has already been established, equation (10) can be rearranged for the bulk pseudo-equilibrium pressure, P_b. This pressure is called the bulk pseudo-equilibrium pressure because the vapor-liquid system is not actually at equilibrium, but the bulk liquid is at an equilibrium state due to the assumption that the entire reaction occurs in the film. After solving the quadratic equation for P_b from equation (10), the bulk concentration of A, B, C are given by

$$c_{A,b} = m_{\text{ethylene Cu}} P_b \tag{14}$$

$$c_{B,b} = c_{\text{Cu total}} - c_{C,b} \tag{15}$$

$$c_{C,b} = c_{\text{total}} - c_{A,b} \tag{16}$$

where $c_{\text{Cu total}}$ is the calculated copper concentration to fit the equilibrium data and not the actual copper concentration.
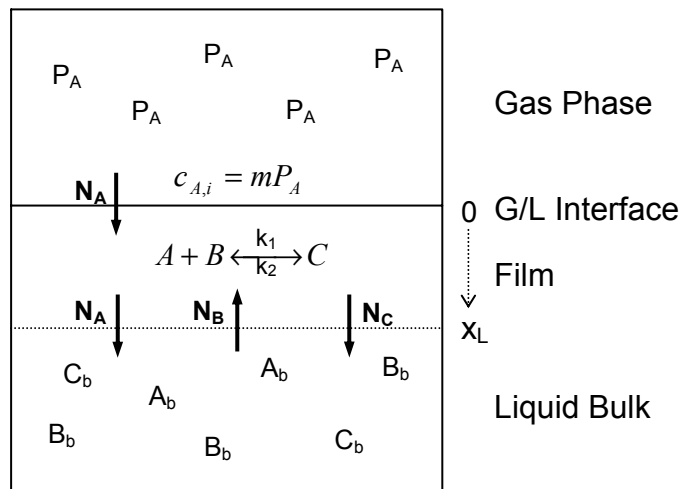

Figure 6. Schematic of gas-liquid concentrations

In order to determine the kinetic effects due to chemical reaction, the enhancement factor is defined as the ratio of the actual rate of ethylene absorption to the rate for strictly physical absorption.

$$\Phi = \frac{R_{\text{observed}}}{R_{\text{physical}}} = \frac{R_{\text{observed}}}{k_L^* a \left(c_{A,i} - c_{A,b} \right)} \tag{17}$$

The observed rate of absorption was calculated at all points throughout the experiment based on change in moles in the gas phase, and the interfacial and bulk ethylene concentrations were found as described previously.

To compare the different models used to describe the kinetic behavior, the reaction rate coefficients and any other adjustable parameters were varied until the model fit the observed rate of absorption at the start of the kinetic experiment. For the reversible, finite rate reaction (13), Onda et al.[10] have developed a method of solution for Φ that can be used to model the absorption rate. The unknown parameters that were adjusted were the forward reaction rate coefficient and the ratio of diffusivities D_B/D_A and D_C/D_A. Since no information was known about the relative diffusivities of the copper-ethylene complex and the uncomplexed copper, the ratios were adjusted simultaneously such that they maintained equal values to one another. The reaction rate coefficient was found to counteract the diffusivity ratio such that a decrease in the diffusivity ratio required an increase in the reaction rate coefficient and vice versa. This relationship is intuitive because the diffusion of material into and out of the reaction film must be balanced by the rate which material reacts in the film. Figure 7 shows the effects of diffusivity ratios of 0.25 and 1 on the fitted reaction rate coefficient (with units of L/mol·s) for the finite, reversible model, where the reaction rate coefficients were adjusted until the calculated rate was equal to the observed rate at time = 0 for each fit.
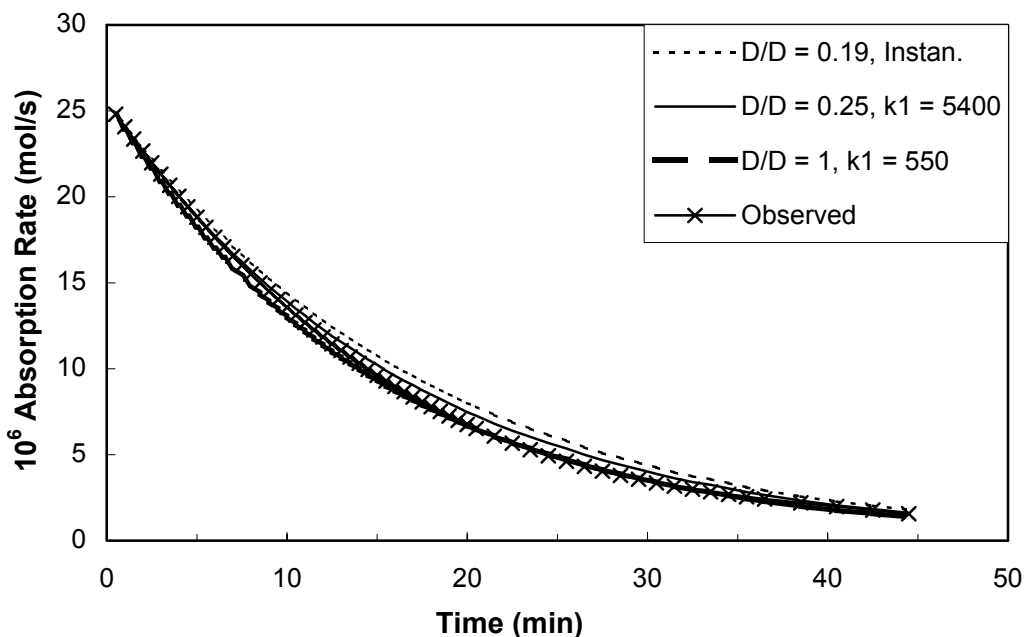

Figure 7. Finite, reversible model fitting parameters

The case where D_B/D_A = 1 showed the closest fit to the observed experimental data; however, it is more reasonable to assume that the copper species will have a lower diffusivity than dissolved, unreacted ethylene. The instantaneous, reversible model in Figure 7 showed an acceptably good fit to the data while allowing only one value for the diffusivity ratio of 0.19. Using the Wilke-Chang equation to estimate the diffusivities gives a ratio of about 0.25, which is close to the value calculated from the instantaneous, reversible model.

Simplifications to the reversible, finite rate model included instantaneous and/or irreversible reaction. The form of each of these simplified models is given in Table 1, and the values of the fitting parameters were found by solutions for the reaction rate developed by Danckwerts.[8] These calculated rates from the various models are shown in Figure 8. From Figure 8, all three irreversible models deviated from the experimental data to a greater extent at longer reaction times. The reversible models followed the appropriate shape of the experimental data throughout the entire range. The finite, reversible case at a reasonable diffusivity ratio required a very high reaction rate coefficient (5400 L/mol·s); therefore, a good approximation was found with the instantaneous, reversible case that also showed an excellent fit to the data.

Table 1. Reaction model form and parameters

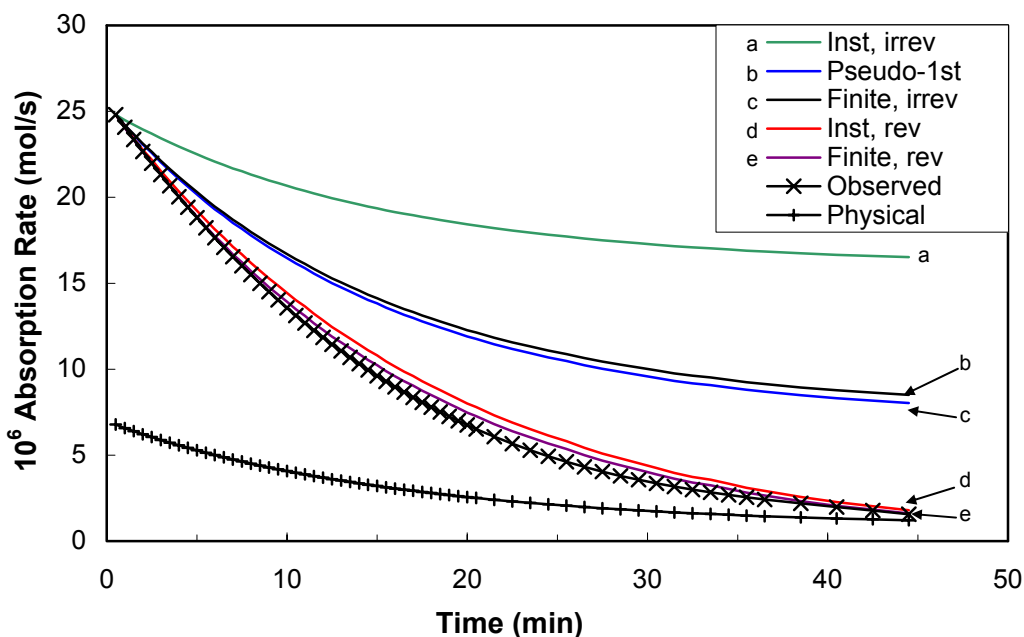| Type	Form	D_B/D_A	k
Inst., irrev.	$A + B \rightarrow C$	0.17	NA
Pseudo-1st	$A \xrightarrow{k_1 B} C$	NA	159 s^{-1}
Finite, irrev.	$A + B \xrightarrow{k_1} C$	0.25	222 L/mol·s
Inst., rev.	$A + B \leftrightarrow C$	0.19	NA
Finite, rev.	$A + B \xleftrightarrow{k_1, k_2} C$	0.25	5400 L/mol·s

Figure 8. Comparison of reaction kinetic models

In comparison to the observed data and the reaction models, the calculated rate of physical absorption from equation (17) is also shown in Figure 8. At the beginning of the experiment the observed absorption rate was much higher than the calculated physical absorption rate with an enhancement factor of 3.66. Near the end of the experiment, the observed absorption rate approached the physical absorption rate leading to enhancement

factors near unity for times over about 40 minutes. At the low stirrer rate used for the kinetic experiments, equilibrium was found to require very long times evident by the very slow approach of the experimental absorption rate to zero. After the rate slowed considerably (at times over about 40 minutes in Figure 8), the stirrer rate was increased to accelerate vapor-liquid equilibrium.

Conclusion

The equilibrium and kinetics of ethylene absorption were investigated with the autoclave apparatus, and the data was found to show good agreement with a simple reaction model that was first-order in ethylene. The equilibrium showed that most of the chemical complexation took place at ethylene partial pressures below about 50 psia. Beyond this point, the equilibrium curve showed the same slope as predicted by physical solubility alone. The capacity of the copper solution for chemical complexation was found to be significantly lower than the actual concentration of copper(I) ions able to form a 1:1 ethylene-copper complex. The selectivity of ethylene to ethane absorption was found to be greatest at lower pressures creating a tradeoff with capacity for the optimum absorption pressure. Both high ethylene capacity and high ethylene to ethane selectivity are preferred, but these two effects act in opposite directions with ethylene pressure.

The modeling of the reaction kinetics showed the reversible models to exhibit the best fit with the experimental data. Due to the close fit of the instantaneous, reversible model, the reaction was assumed to be very fast, and the diffusivity ratio D_B/D_A was estimated to be 0.19. Further work that would lend validity to this model would be to experimentally find the diffusivity of the ethylene-free copper(I) species in solution. Another recommendation for future work is to perform the autoclave equilibrium experiment on a sample of a mixed ethylene-ethane stream from an actual industrial process stream. Repeated experiments should confirm that the absorption solution is robust enough to handle the impurities present before attempting implementation on a larger scale.

Nomenclature

a	interfacial mass transfer area
c	solute concentration in liquid
$c_{chemical}$	concentration of ethylene in solution solely due to chemical absorption
c_{total}	total concentration of ethylene in solution due to both physical and chemical absorption
$c_{Cu\ total}$	total copper concentration
D_i	diffusivity of solute i in liquid solution
k	reaction rate coefficient
K_{eq}	equilibrium constant
k_L^*	physical mass transfer coefficient
m	Henry's law constant for physical solubility
n	number of moles
N_i	molar flux of component i
P	pressure
R	gas constant
R_j	rate of reaction or mass transfer
T	temperature
V	volume
x_L	length of liquid film where reaction and diffusion occur
Z	compressibility factor
Φ	enhancement factor

Superscripts and subscripts

$*$	denotes equilibrium condition
1	denotes forward reaction rate
2	denotes reverse reaction rate
A,B,C	denotes component
b	denotes bulk condition
i	denotes interfacial condition

References

1. Gerhartz, W., Ed. Ethylene. *Ullman's Encyclopedia of Industrial Chemistry*. 5th edition. VCH Verlagsgesellschaft: Weinheim, 1987, Vol. A10, pp 45-93.
2. Humphrey, J.L.; Seibert, A.F.; Koort, R.A. Separation Technologies Advances and Priorities. U.S. Dept. of Energy Report 12920-1, 1991.
3. Eldridge, R.B. Olefin/Paraffin Separation Technology: A Review. *Ind. Eng. Chem. Res.* 1993, 32, 2208-2212.
4. Jamal, A.; Meisen, A. Kinetics of CO induced degradation of aqueous diethanolamine. *Chem. Eng. Sci.* 2001, 56, 6743-6760.
5. Kim, C.J.; Palmer, A.M.; Milliman, G.E. Absorption of Carbon Monoxide into Aqueous Solutions of K_2CO_3, Methyldiethanolamine, and Diethylethanolamine. *Ind. Eng. Chem. Res.* 1988, 27, 324-328.
6. Smith, J.M.; Van Ness, H.C.; Abbott, M.M. *Introduction to Chemical Engineering Thermodynamics*, 5th ed.; McGraw-Hill: New York, 1996.
7. Laddha, S.S.; Diaz, J.M.; Danckwerts, P.V. The N_2O Analogy: the Solubilities of CO_2 and N_2O in Aqueous Solution of Organic Compounds. *Chem. Eng. Sci.* 1981, 36, 228-229.
8. Danckwerts, P.V. *Gas-Liquid Reactions*. McGraw-Hill: New York, 1970.
9. Xu, S.; Wang, Y.; Otto, F.D.; Mather, A.E. Kinetics of the Reaction of Carbon Dioxide with 2-Amino-2-methyl-1-propanol Solutions. *Chem. Eng. Sci.* 1996, 51, 841-850.
10. Onda, K.; Sada, E.; Kobayashi, T.; Fujine, M. Gas Absorption Accompanied by Complex Chemical Reactions – I. Reversible Chemical Reactions. *Chem. Eng. Sci.* 1970, 25, 753-760.